ELSEVIER

Physica E 13 (2002) 89–93

PHYSICA E

www.elsevier.com/locate/physe

A novel split gate design to study interaction effects in quantum wires

M. Tornow [1], M. Heiblum *, D. Mahalu, H. Shtrikman, V. Umansky

Braun Center for Submicron Research, Department of Condensed Matter Physics, Weizmann Institute of Science, Rehovot 76100, Israel

Received 6 May 2001; accepted 7 June 2001

Abstract

A new concept to form ballistic quantum wires based on a triple split gate structure on top of a GaAs/AlGaAs heterostructure is presented. Due to the flexibility in the design we propose this method, which would allow one to check the predictions of the Luttinger liquid model. The current–voltage characteristic of an embedded tunneling barrier in a 2 μm long ballistic quantum wire is also addressed in some detail.

PACS: 73.23.Ad; 73.63.Nm

Keywords: Quantum wires; Ballistic transport; Electron interactions

A major part of the growing interest in strongly correlated electron systems concentrates on a better understanding of interacting electrons in one dimension (1D), exhibiting non-Fermi liquid behavior. Well established in theory, such a system should rather be described—even for arbitrarily weak interactions—as a so-called Luttinger liquid (LL) (for reviews see, e.g., Refs. [1–3]). Spatial correlation among the electrons, which increases with decreasing temperature, gives rise to various remarkable properties [4]. For example, the Drude conductance of an infinitely long LL with only a single impurity is predicted to be suppressed according to a power law as a function of applied voltage (V) and temperature (T) (non-linear I–V), eventually vanishing at $V=0$, $T=0$. This behavior arises from the zero tunneling density of states for electrons for $V=0$ at $T=0$.

For an unambiguous study of the predictions an extremely clean 1D system (quantum wire, QWR) is highly desirable, since the presence of even a small residual disorder may largely obscure the desired observation of interaction effects. Due to the difficulty of preparing suitable QWRs, only a few experiments addressing the theoretical predictions were reported

* Corresponding author. Alex and Ida Sussman Professional Chair in Submicron Electronics. Fax: +972-8-934-4128.

E-mail address: heiblum@wisemail.weizmann.ac.il (M. Heiblum).

[1] Present address: Walter Schottky Institut, Technische Universität München, D-85748 Garching, Germany.

1386-9477/02/$ - see front matter
PII: S1386-9477(01)00229-6

(see, e.g., Refs. [5,6]). More recent results on carbon nanotubes and chiral edge states in the fractional quantum Hall effect regime could be interpreted in a satisfactory manner within the LL picture [7,8]. Deviating from ideality, for example, in a recent work [9] on very lightly disordered wires, fabricated on a cleaved edge of a 2D system, tunneling through a natural island within the wire was investigated. The observed temperature dependence of the Coulomb Blockade peaks could be successfully explained within the LL picture.

In the present work, we introduce a new concept: a multi-gate configuration, which forms a high quality QWR with an added flexibility. For example, an easy introduction of a potential barrier along the wire is possible. After describing our novel split gate design and presenting representative measurements on a 0.5 μm long QWR, first results on the tunneling through a barrier in a 2 μm long QWR device will be described.

The preparation of our QWRs is based on the widely used technique of laterally confining a high mobility two-dimensional electron gas (2DEG), at the interface of an AlGaAs/GaAs heterostructure, to a narrow one-dimensional channel by using deposited split gates. The main new component is a third gate put in between the two negatively biased, channel limiting, gates. This “middle gate”, only some 20–30 nm wide, is biased positively. This configuration, combined with the very small distance measured from the 2DEG to the surface, allows a narrow lateral confinement while retaining a high density 1D electron gas.

The steep potential walls lead to a larger subband splitting, which reduces the inter-subband scattering.

We report the results measured on two samples made from two different starting materials, both prepared from MBE-grown GaAs/AlGaA s heterostructures, containing shallow high mobility 2DEG. In sample A, the distance of the 2DEG to the surface is $d = 50$ nm, the electron mobility is about $\mu = 10^6$ cm^2/V s at a density of $n_s = 2.7 \times 10^{11}$/cm^2 measured at $T = 4.2$ K in the dark. In sample B, $d = 53$ nm and $\mu = 1.7 \times 10^6$ cm^2/V s at $n_s = 3.7 \times 10^{11}$/cm^2. The metallic gates were formed by means of high resolution e-beam lithography (200 nm double layer PMMA), UHV evaporation of a standard AuPd (80/20) alloy and a subsequent lift-off process. Metal line widths and spacings were as small as 20 nm, but typical dimensions of lines were 30 nm and spacings were 80 nm. Proximity effects during the e-beam writing were drastically reduced via using metal lines instead of large metal pads for the side gates. Conductance measurements were performed at temperatures between 400 mK and 4.2 K by applying an AC voltage $V_{AC} = 10$–100 μV to the drain (source

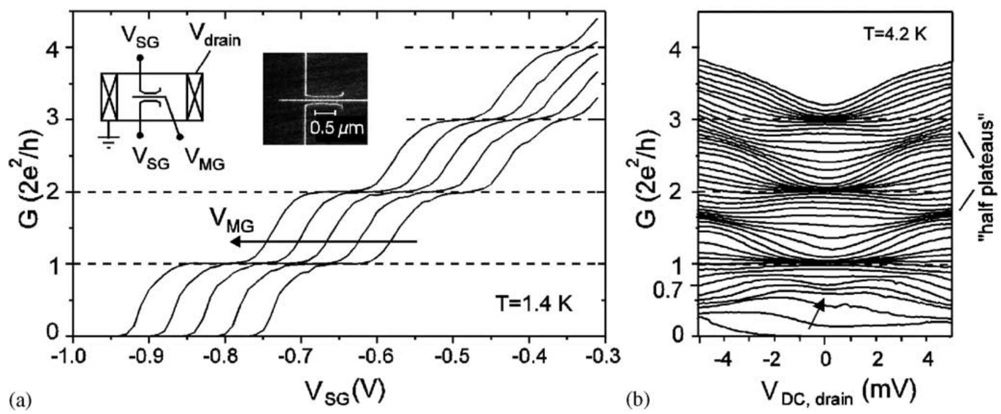

Fig. 1. (a) Conductance of a 0.5 μm long quantum wire (sample A) as a function of side gate voltage V_{SG} at $T = 1.4$ K, measured with an excitation voltage $V_{AC} = 100$ μV. Different curves correspond to different positive middle gate voltages $V_{MG} = 0.25$–0.45 V from right to left. Inset left: Schematic view of the sample setup, crossed rectangles assign ohmic contacts. Inset right: SEM picture showing the AuPd split gates of the central device region. Note, that the length 0.5 μm refers to the strictly parallel section of the gates, not including the smooth openings. Other geometrical dimensions are approximately linewidth 30 nm, line spacing 200 nm between side gates. (b) Differential conductance for the sample of Fig. 1(a) at fixed $V_{MG} = 0.35$ V and $T = 4.2$ K. Different curves correspond to V_{SG} from −0.50 V (top) to −0.96 V (bottom) in steps of −0.01 V. The arrow points to a non-linear conductance regime, indicating the so-called “0.7 structure”.

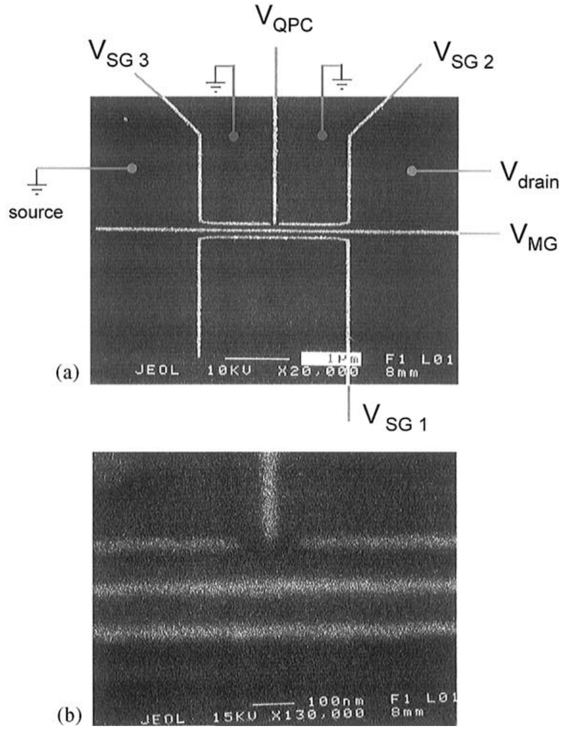

Fig. 2. (a) SEM picture of a 2 μm QWR device with a center QPC. The five split gates at the surface of the AlGaAs/GaAs heterostructure (compare inset of Fig. 1(a)) can be biased with individual voltages. For details of the device operation see text. The 2DEG regions between V_{SG2} and V_{SG3} remain grounded to avoid floating conductive planes close to the wire. (b) Detail view of the center of (a).

was grounded). Up to a few mV, DC voltage wast added to the drain in order to extract the full range differential conductance.

Fig. 1 shows the conductance of a 0.5 μm long QWR (sample A) made by a triple gate design as seen in the inset. While the two side gates were biased negatively with V_{SG}, the QWR in between the gates is formed as a result of biasing the middle gate with a positive voltage V_{MG}. All conductance measurements were done after verifying that the leakage currents in the gates, especially in the middle gate, were typically less than 20 pA at 4.2 K. Fig. 1(a) shows the lowest, well pronounced, quantized 1.4 K conductance steps of the QWR as a function of V_{SG} with V_{MG} as a parameter. Note that no correction for the lead resistance (and Ohmic contacts) was done since it was very small. With increasing V_{MG}, the 1D density in the channel increased. Consequently, the characteristic voltage range of V_{SG}, down to pinch-off, shifted to more negative voltages and at the same time the plateaus were better resolved (due to the suppressed scattering). We observed conductance quantization up to wire lengths of 2 μm in similar devices.

For the study of interaction effects in 1D, measurements of the differential conductance is of particular interest. Fig. 1(b) shows, for the same device presented in Fig. 1(a), the conductance as a function of an added DC source–drain voltage, $V_{DC,drain}$, for a series of V_{SG} voltages at a fixed value of V_{MG}. Closer to $V_{DC,drain} = 0$ the curves merge with the lowest 3 quantized conductance plateaus. The quantization disappears when $V_{DC,drain}$ becomes the order of the level separation; then the number of conducting subbands for the two directions of transport differs by one. Under these conditions the so-called "half plateaus" (Ref. [10] and references therein) evolve. Their value, rather than being exactly quantized, depends on the voltage drop at the constriction. For a partially transmitted first channel, which will be the focus of our study, various effects must be taken into account, which may complicate the interpretation. First, the differential conductance traces below $G = 2e^2/h$ become non-symmetric with respect to $V_{DC,drain}$ (compare with Refs. [10,11]). Second, many investigated devices (including sample A) show "random telegraph noise" near pinch-off, i.e., the conductance is unstable between two or more values. Finally, the I–V characteristic is non-linear for small biases. Here, we find an indication of the recently discussed "0.7 structure" [11,12] in Fig. 1(b) (arrow).

The rest of the paper will focus on the question of tunneling of interacting 1D electrons through a 1D potential barrier. The conductance of a (infinitely long) QWR, perturbed by a large potential barrier, is predicted to follow a power law [4]:

$$G(V) = \mathrm{d}I/\mathrm{d}V \propto |t_0|^2 |V|^{(2/g)-2}, \qquad (1)$$

where t_0 denotes the (bare) transmission amplitude. The Luttinger interaction parameter g equals 1 for the non-interacting case and then yields a linear I–V curve. Repulsive interaction ($g < 1$) results in a zero conductance for $V \to 0$ at zero temperatures. However, the conductance of QWRs of finite length L is

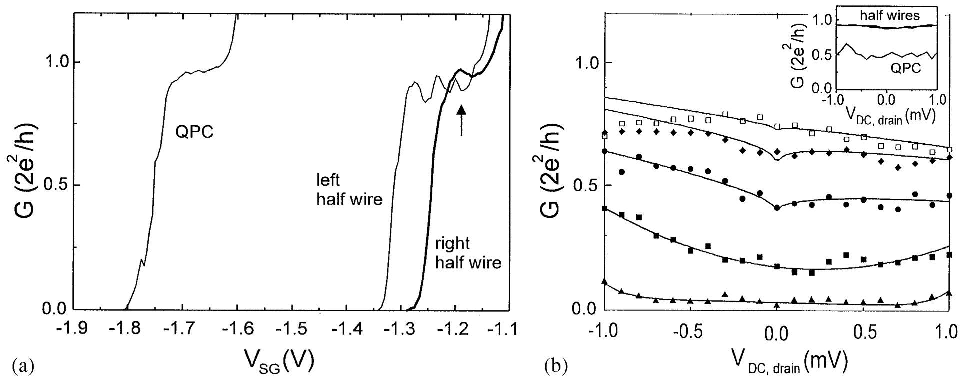

Fig. 3. (a) Conductance of the quantum wire device (sample B) of Fig. 2 at $T \approx 400$ mK, $V_{AC} = 10$ μV, $V_{MG} = +250$ mV: Lowest ($n = 1$) quantized conductance plateaus of the QPC only, the left half wire (using SG3) and the right half wire (using SG2), see Fig. 2(a). The arrow denotes the voltage value $V_{SG1,2,3} = -1.19$ V in the overlap region of the $n = 1$ plateaus of the two half 1 μm wires. (b) Averaged (10×) differential conductance data for the same device. For all traces $V_{SG1,2,3} = -1.19$ V. V_{QPC} varies from −1.85 V (top, open squares) to −2.05 V (bottom, full triangles) in steps of −0.05 V. Thin full lines: $G(V) = A + B|V/V_0|^{(2/g)-2} + C|V/V_0|$ with $V_0 = 1$ mV (cp. Eq. (1)). From top to bottom $g = 0.98, 0.9, 0.8, 0.5$ and 0.2. A, B and C (C to compensate for the slight asymmetry) were adjusted individually for best visual fits of the data points. Inset: The two 1 μm wire halves at the 1st plateau measured separately at $V_{SG1,2} = -1.2$ V and $V_{SG1,3} = -1.2$ V, respectively, and the quantum point contact alone at $V_{QPC} = V_{SG1} = -1.725$ V.

expected to saturate at a finite value once the corresponding "thermal length" $hv_F/2\pi k_B T$, or voltage related length $hv_F/2\pi eV$, exceeds L (v_F: 1D Fermi velocity). For example, a 2 μm long QWR, transmitting the $n = 1$ channel, with electrons' Fermi energy of 3 meV will have a saturated conductance at $V = 40$ μV and $T = 470$ mK. In our experiments, with the 2 μm long QWR device we used $V_{AC} = 10$ μV and $T \approx 400$ mK. If the applied voltage and temperature are kept within the "saturated regime", we would expect to observe a maximum change in differential conductance.

We prepared a 2 μm long triple gate QWR, which contains a tunable quantum point contact (QPC) at its center. The various modes of operation, as a function of the multiple split gates are best explained with the help of Fig. 2. In the picture, one recognizes the three main gate lines that form the wire, namely, the bottom side gate (V_{SG1}), the middle gate (V_{MG}) and the top side gate, which is now split into two independent halves (V_{SG2}, V_{SG3}). In between the two top side gates, an additional finger-like side gate (V_{QPC}) enters, acting as a QPC. The various modes of operation are (1) Grounding gates SG2 and SG3, allowing an operation of the QPC alone. This enables the study of transport between two 2DEGs (Fermi liquids). (2) Biasing one side gate SG2 (or SG3), and leaving the other one (and the QPC) grounded, leads to a single 1 μm long QWR. (3) Operating the "whole device", i.e., biasing SG2 and SG3 as well as the QPC individually in order to investigate a 2 μm long locally perturbed QWR. This leads to tunneling between two Luttinger liquids through their edges. Other combinations are possible, but will not be discussed here. We note that a bare 2 μm long, totally unperturbed QWR cannot be formed with this design.

Results of measurements with this device (sample B) are presented in Fig. 3. At first, in order to find the correct gate voltage biases, needed to adjust the split QWR, such that only the first channel is transmitted, the conductance of the 1 μm long QWR was measured. Conductance of two such wires, "left", with SG3, and "right", with SG2, are shown in Fig. 3(a). An oscillating structure, which probably originates from transmission resonances and scatterers inside the wire, is visible on top of the conductance plateau. In order to operate both 1 μm long wires in series, biasing conditions of the gates marked by the arrow in Fig. 3(a) were chosen. Also included in Fig. 3(a) is the lowest plateau of the QPC alone, which, as expected from the design (compare with Fig. 2(b)), needs a much larger negative voltage to pinch-off.

We finally address the differential conductance, which is smaller than the quantum conductance. Due to large fluctuations of the conductance at a fixed V_{SG} near pinch-off, which increase in amplitude with increasing $V_{DC,drain}$, we averaged the differential conductance data over many subsequent scans. We first checked the conductance of the QPC and the individual 1 μm long QWRs as reference. The inset of Fig. 3(b) shows the data of the differential conductance. For both individual 1 μm long QWRs, at $n=1$, G is constant as a function of $V_{DC,drain}$ within a few percent. The QPC alone at about $0.5 \times 2e^2/h$ exhibits a similar behavior. In contrast, the conductance of the 2 μm long "whole device", below $2e^2/h$, reveals a weak but characteristic dependence on $V_{DC,drain}$. Fig. 3(b) displays five differential conductance traces. For each of them the gate bias of the QPC is different, while both half QWRs are being retained at $n=1$. For large QPC potential barriers, the differential conductance as a function of $V_{DC,drain}$ can be qualitatively described by power law dependencies as in Eq. (1), however, with a V_{QPC} dependent interaction parameter, $g(V_{QPC})$. Using large and small QPC transmission values given by the shown conductance traces, we find that $g=0.98$ (high transmission, top), 0.9, 0.8, 0.5 and 0.2 (small transmission, bottom). We note that a decreasing value of g might result from a decrease in 1D electron density (e.g., Ref. [4]). This is possible in the wire region closer to the QPC for large QPC barriers. A further, less ambiguous interpretation, however, within the framework of the Luttinger liquid model, remains beyond the scope of these measurements.

In summary, we present a new technique to prepare quantum wires in order to check the predictions of the transport of interacting electrons in 1D (Luttinger liquid). Introducing a third, positively biased centered gate, along the length of the wire, proves to generate a robust quantization as demonstrated in a 0.5 μm long quantum wire. Making use of the flexibility of our design, we prepared a 2 μm long wire sample with a tunable quantum point contact in its center. Adjusting the transmission of the first channel, we studied the tunneling of 1D electrons through a barrier. Preliminary measurements of the differential conductance are in qualitative agreement with the predicted power law with a barrier height dependent interaction parameter g.

Acknowledgements

M.T. acknowledges financial support from a MINERVA fellowship. The work was partly supported by the GIF foundation and the MINERVA foundation. We would like to thank A.M. Finkel'stein for useful discussions.

References

[1] M.P.A. Fisher, L.I. Glazman, in: L.L. Sohn, L.P. Kouwenhoven, G. Schön (Eds.), Mesoscopic Electron Transport, Nato ASI Series E, Vol. 345, Kluwer, Dordrecht, 1997.
[2] H.J. Schulz, in: E. Akkermans, G. Montambaux, J.-L. Pichard, J. Zinn-Justin (Eds.), Mesoscopic Quantum Physics, Elsevier, Amsterdam, 1995.
[3] J. Voit, Rep. Prog. Phys. 57 (1994) 977.
[4] C.L. Kane, M.P.A. Fisher, Phys. Rev. B 46 (1992) 15233.
[5] S. Tarucha, T. Honda, T. Saku, Solid State Commun. 94 (1995) 413.
[6] A. Yacoby, H.L. Stormer, N.S. Wingreen, L.N. Pfeiffer, K.W. Baldwin, K.W. West, Phys. Rev. Lett. 77 (1996) 4612.
[7] M. Bockrath, D.H. Cobden, J. Lu, A.G. Rinzler, R.E. Smalley, L. Balents, P.L. McEuen, Nature 397 (1999) 598.
[8] A.M. Chang, L.N. Pfeiffer, K.W. West, Phys. Rev. Lett. 77 (1996) 2538.
[9] O.M. Auslaender, A. Yacoby, R. de Picciotto, K.W. Baldwin, L.N. Pfeiffer, K.W. West, Phys. Rev. Lett. 84 (2000) 1764.
[10] N.K. Patel, J.T. Nicholls, L. Martin-Moreno, M. Pepper, J.E.F. Frost, D.A. Ritchie, G.A.C. Jones, Phys. Rev. B 44 (1991) 13549.
[11] A. Kristensen, H. Bruus, A. Forchel, J.B. Jensen, P.E. Lindelof, M. Michel, J. Nygard, C.B. Sorensen, ICPS24, Jerusalem, August 1998.
[12] K.J. Thomas, J.T. Nicholls, M.Y. Simmons, M. Pepper, D.R. Mace, D.A. Ritchie, Phys. Rev. Lett. 77 (1996) 135.